THE JOURNAL OF COMPARATIVE NEUROLOGY 298:97–112 (1990)

Demonstration of Discrete Place-Defined Columns—Segregates—in the Cat SI

OLEG V. FAVOROV AND MATHEW E. DIAMOND
Departments of Physiology and Endodontics, The University of North Carolina at Chapel Hill, Chapel Hill, North Carolina 27599-7545

ABSTRACT

The SI forelimb area of cats was examined with receptive field (RF) mapping techniques. Arrays of closely spaced, near-radial microelectrode penetrations were inserted into the crown of postsigmoid gyrus of ketamine anesthetized subjects and minimal RFs were obtained at several depths. The minimal RF was defined as the skin site providing the strongest input to each recorded cluster of neurons. Data analysis showed that all studied cortical territories contained groups of discrete cortical columns, 300–400 μm in diameter. The columns were regarded as topographic entities because no change in minimal RF location could be observed within their boundaries. The boundaries of columns were sharp and could be unequivocally distinguished because the minimal RFs sampled on opposite sides of a boundary occupied displaced, nonoverlapping positions.

Pair-wise comparison of single neuron maximal RFs (defined as the entire skin area providing input to the recorded neuron) further clarified the nature of the SI place-defined columns: (1) no *systematic* differences in maximal RF position could be demonstrated for different parts of the same column (even though the maximal RFs in most columns varied extensively in size and skin areas covered), and (2) at the boundary between neighboring columns maximal RFs shifted en masse to center on a new skin locus. These minimal and maximal RF observations strongly support our recent proposal that body surface is represented in SI by a honeycomblike mosaic of discrete place-defined cortical columns, segregates.

Key words: cortex, somatosensory, somatotopy, receptive field, tactile

Powell and Mountcastle ('59) provided the earliest evidence that cutaneous regions of primary somatosensory cortex (SI) may contain discrete columns defined by the location of the receptive fields (RFs) of their constituent neurons. They observed that on many occasions when a recording electrode was advanced for relatively large distances in the anteroposterior direction through the monkey's area 3b, the RFs of successively recorded neurons did not move progressively but remained "confined fairly well to the same skin region" (p. 153). They also pointed out that the RFs "shifted suddenly" after traversing a region in which little or no RF shift was detected (p. 154), suggesting that a boundary separating columns receiving inputs from different skin sites had been crossed. Although these observations were reported over three decades ago, a number of factors have made the experimental demonstration of discrete place-defined SI columns less than straightforward, and these factors prevented until recently (Favorov et al., '87; Favorov and Whitsel, '88a) a systematic mapping of SI columnar units defined on the basis of RF locus. First, because the RFs of single SI neurons (even those that are neighbors) can vary significantly in size and shape (Iwamura et al., '85; Favorov et al., '87; Favorov and Whitsel, '88a,b), no single RF is representative of the RFs of all neurons at any given cortical location. This fact makes it necessary to sample the RFs of a sizeable number of neurons, if one is to adequately characterize the RFs of the neurons at any SI location. This requirement, in turn, raises a second difficulty: only a limited fraction of single neurons that are present in a given column can be isolated and studied in the course of a microelectrode penetration. In our view, the prominent RF variability that exists in normal SI cortex and the limited RF sampling have prevented previous investigators of SI topographical organization from observing discrete place-defined columns and led them to conclude that when travelling across the SI cortex, the RFs gradually shift on the skin in a partially overlapping, essentially continuous manner. The extensive series of RF mapping studies published by our laboratory reflects

Accepted May 17, 1990.

Address reprint requests to Dr. O. Favorov, Department of Physiology, The University of North Carolina, Chapel Hill, NC 27599-7545.

M.E. Diamond is now at the Division of Biomedical Science, Brown University, Providence, RI 02912.

this point of view quite clearly (see McKenna et al., '81, '82 for reviews).

Recently, Favorov and Whitsel ('88a) found, in a study of area 1 of *Macaca fascicularis* monkeys, that the difficulties in identifying columnar aggregates based on RF locus can be circumvented by: (1) inserting penetrations at a sharp angle to the radial cell cords (near-radial penetrations), thus increasing the number of single neurons sampled per unit distance in the tangential cortical plane, and (2) determining the skin area common to the RFs of sequences of individual SI neurons sampled in such a penetration. The authors found that their results were most consistent with the view that with regard to its skin input, the monkey's area 1 is organized as a mosaic of distinct, nonoverlapping columns, 0.6 mm in diameter. According to this hypothesis, orderly, systematic shifts of the RF position are absent within such columns, although RFs of neighboring neurons can differ prominently in their position on the skin. It is only at a moment of crossing the boundary separating two adjacent columns, that RFs shift en masse to a new, but partially overlapping the old, skin territory. Because of their prominent diversity, the RFs of the neurons comprising a column share only a very small skin locus in common. This shared skin locus can be used to distinguish neighboring columns, because the shared skin loci of neighboring columns are prominently displaced, nonoverlapping, and noncontiguous with each other. These place-defined columns were named "segregates."

In addition to the single-unit RF mapping method, SI has also been extensively studied with the use of the multiunit, or cluster, recording method, usually in deeply anesthetized preparations. Two distinctive features of the RFs mapped using this recording method and conditions are (1) their small size, and (2) uniformity of the RFs mapped at different depths in a radial penetration (Merzenich et al., '78; Nelson et al., '80). Although abrupt shifts in the position of multiunit RFs sampled at nearby loci (termed "discontinuities") have been widely reported (for review see Kaas et al., '81; Merzenich et al., '81; see also Dykes and Gabor, '81), such discontinuities are encountered much less frequently than the discontinuities—the segregate boundaries—reported by Favorov and Whitsel ('88a). For example, the former do not occur within relatively large sectors of SI; instead, series of multiunit recording sites sampled within such large regions yield series of partially overlapping, gradually shifting RFs.

We recently (Favorov et al., '87) found that an appropriately modified multiunit recording and RF mapping method can be used to estimate the skin locus shared in common by the maxRFs of a given segregate (for details see Methods). Our approach was to use the method to identify the skin locus whose stimulation evokes the *strongest* neuroelectrical activity at a given recording site. Accordingly, we used very gentle (near-threshold) punctate tactile stimuli and mapped the skin area from which such a stimulus evoked the strongest response at each recording site in deeply anesthetized animals. Because these procedures minimize the size of the mapped RF, the method was assigned the name the "minimal receptive field" (minRF) mapping method. This method was successfully applied in the course of near-radial penetrations of area 3b in the cat (Favorov et al., '87). Specifically, when sequences of minRFs were obtained at 100–150 μm intervals along a slightly tilted electrode track, they revealed, without a single exception, a steplike progression of minRFs on the skin. That is, although strings of nearly identical minRFs were mapped at a number of consecutive recording sites, these were typically followed by an abrupt shift of the minRF to a new, nonoverlapping position. In a series of penetrations that combined both the maxRF and minRF methods, we found that the minRF obtained within a given segregate matched the skin locus shared in common by the maxRFs sampled in that same segregate (Favorov et al., '87). Furthermore, abrupt shifts of minRF occurred at the same cortical locations where the boundary separating two segregates was detected with maxRF method. Thus it was our conclusion that both the maxRF and minRF methods can detect the same discrete place-defined columns in SI and that the minRF method can be used as an efficient substitute for the much more time-consuming maxRF method.

Our published studies in the cat and monkey have relied primarily on the analysis of sequences of RFs mapped in single penetrations. These data are limited, of course, for they provide only indirect information about the spatial dimensions of SI segregates. Furthermore, RF data collected in single penetrations are not well suited for distinguishing between two possible plans of topographic organization: (1) a honeycomblike pattern of small diameter columns, each of which lacks internal somatotopy (i.e., the segregate organization we proposed), and (2) a pattern of highly irregular, convoluted bands, each organized somatotopically along its long axis, like the organization proposed for the bands of slowly and rapidly adapting neurons in area 3b (see Sretavan and Dykes, '83; Sur et al., '84). To address these issues, minRF data were collected in arrays of closely spaced penetrations. These new data, as well as quantitative analyses of maxRF data collected in earlier experiments (Favorov et al., '87), constitute the results of this study. Our purpose is twofold: (1) to provide further evidence for the existence of segregates in the cat SI, and (2) to provide a detailed description of the segregate organization present in this cortical field. Two particular aspects of segregate organization are addressed: (1) the shape and size of segregates, and (2) the characteristics of the individual maxRFs sampled within a segregate. The data were collected in studies of the forelimb region of cytoarchitectonic areas 3b and 1 in cats. Because the RFs mapped in areas 3b and 1 were indistinguishable both in the present series of experiments and in the experiments of others (Dykes et al., '80; McKenna et al., '81; Felleman et al., '83), the data from the two cytoarchitectonic areas were not treated separately. The study was restricted to those cortical territories that received cutaneous peripheral input in order to avoid technical complications that would be involved in accurate mapping of deep RFs.

METHODS

The receptive field data described in this study were collected under two different experimental conditions and using two different RF mapping methods—maxRF (maximal receptive field) and minRF. The maxRF data were collected in an earlier series of experiments (Favorov et al., '87; see also Favorov and Whitsel, '88a for methodological details). The maxRF mapping method is described in great detail in our earlier publications; therefore, only a limited description of the method is provided here.

General preparation

In all subjects general anesthesia was induced using a mixture of 1–3% halothane in oxygen, and a recording chamber was installed over the forelimb region of the SI. All surgical sites were infiltrated and topically dressed with Dibucaine ointment.

In those experiments in which the minRF method was to be used, the gaseous anesthetic was discontinued, ketamine hydrochloride (15 mg/kg, IM) was administered, neuromuscular block was induced with gallamine triethiodide, and the subjects were respired using positive pressure ventilation. The rate and volume of respiration were continuously adjusted to maintain end-tidal CO_2 between 3.5 and 4.5%. Supplemental doses of ketamine were given to maintain a level of general anesthesia ensuring complete insensitivity to all environmental stimulation (assessed continuously by the slow wave content of the EEG).

In those experiments in which the maxRF method was to be used, neuromuscular block was induced and subjects were ventilated with a 50:50 mixture of nitrous oxide and oxygen immediately after withdrawal of the halothane in oxygen anesthetic. Subjects were placed in a recumbent position on a padded table and at least 2 hours were allowed for complete elimination of the halothane anesthetic before beginning the maxRF mapping. These conditions and the practices we employed to map maxRFs do not lead to the autonomic (e.g., elevation in blood pressure, changes in pupilary status, etc.) or neurophysiological signs (changes in EEG status) characteristic of stress or pain (Whitsel et al., '72; Bennett et al., '80; Weinberger et al., '84; unpublished observations).

Neurophysiological and RF mapping methods

Extracellular recordings were obtained under closed chamber conditions using electrolytically sharpened, glass-insulated tungsten electrodes (impedance 200–400 Kohm at a test frequency of 10 KHz, exposed at the tip by passing current through the microelectrode). The very small recording radius of the electrodes (typically 20–50 μm; Favorov and Whitsel, '88a) allowed a high rate of sampling of single units (on average 1 per 100 μm).

The study was restricted to cortical territories that received cutaneous peripheral input. Accordingly, when a penetration passed through a cortical column whose neurons had deep RFs, the occurrence and location of such neurons were noted in protocols and the penetration was continued until neurons having cutaneous RFs or white matter were encountered. Maximal RFs were mapped for single neurons isolated on the basis of the amplitude and the shape of the recorded action potentials. The stimulus that evoked the most vigorous response from the recorded neuron when applied to the most sensitive part of the RF was selected as the mapping stimulus. The entire, or maximal, skin field from which spike discharge activity was evoked in the recorded neuron was then included in the maxRF. Nociceptive stimuli were never delivered.

Minimal RFs were mapped using the amplified and unfiltered neuroelectrical activity recorded by the electrode. The unique version of minimal RF mapping method employed in this study was designed for (1) identification of the very small skin area that is shared in common by the maxRFs of all the single neurons comprising a given segregate, and (2) detection of the boundary separating neighboring segregates. As was shown in our earlier work (Favorov et al., '87), these two goals can be easily achieved using an RF mapping method that identifies the physiological center of the RF of a local neuron cluster. In particular, our minRF mapping method relies on use of deep general anesthesia and near-threshold von Frey filaments to reduce the size of the mapped RF to its minimum at its most sensitive, most effective skin locus. At the dosage of ketamine used in the present study, there is a significant reduction of the size of the mapped RF, but only a relatively minor loss of neuron's normal sensitivity to skin contact in the central portions of their RFs (McKenna et al., '81; Duncan et al., '82; Chapin and Lin, '84). The most effective skin locus was further pinpointed by two approaches: (1) by using the weakest von Frey filament that consistently evoked a distinguishable response, and (2) by identifying the skin field that, when stimulated with a near-threshold von Frey filament, evoked the most vigorous response. In addition, we attempted to limit the effective sampling radius of the recording electrode, because the larger the volume of cortex "seen" by the electrode, the more likely that neurons lying in neighboring segregates would contribute to the recorded activity. Accordingly, a large-tipped, "open" electrode was expected to obscure discrete topographic boundaries and give the impression that RFs shift gradually and continuously (for more detailed discussion of this problem, see Favorov and Whitsel, '88b). Based on this rationale, we mapped minRFs using the same type of recording electrode that we have used to obtain single-unit recordings from the SI cortex. Based on the observations described in Results, we estimate that such fine-tipped electrodes pick up neuroelectric activity limited to cortical regions located 30 μm or less from the electrode tip.

A final aspect of the unique minRF mapping technique employed in this study is that we sought to avoid, whenever possible, the presence in the recordings of neuroelectrical activity of spikes of large amplitude (i.e., when the recording revealed one or several units with action potentials much larger than those of the rest of the recorded neuronal population, the electrode was moved slightly in an attempt to reduce the amplitude of the large units). This action was taken because it was recognized early in the study that minRFs mapped using recordings that contained such prominent single units frequently had larger than usual sizes and showed more variability in their position on the skin (for example, see Fig. 5). Apparently, minRFs mapped in the presence of one or several single units with large spikes were unduly weighted by those single units. As a result, the minRFs reflected the variations in the size and position of the RFs of those single units. Such prominent variations in single neuron RFs were evident even under the condition of deep general anesthesia.

A certain degree of inaccuracy and subjectiveness is inherent in mapping RF outlines, unless it is done using computer-controlled mechanical stimulators. Although the accuracy of RF mapping was essential for the purposes of this study, such an approach would have been prohibitively time-consuming. To improve the accuracy of mapping RFs by hand, the following four procedures were adopted. First, in each experiment prior to the RF mapping session, a fine grid of reference lines was drawn on the shaved skin of the forelimb (using consistently identifiable morphological features for orientation). These lines served to increase the accuracy of placement of the RF boundaries mapped during the experiment. Second, each RF was plotted on a drawing of the unfolded surface of the forelimb, which had the same

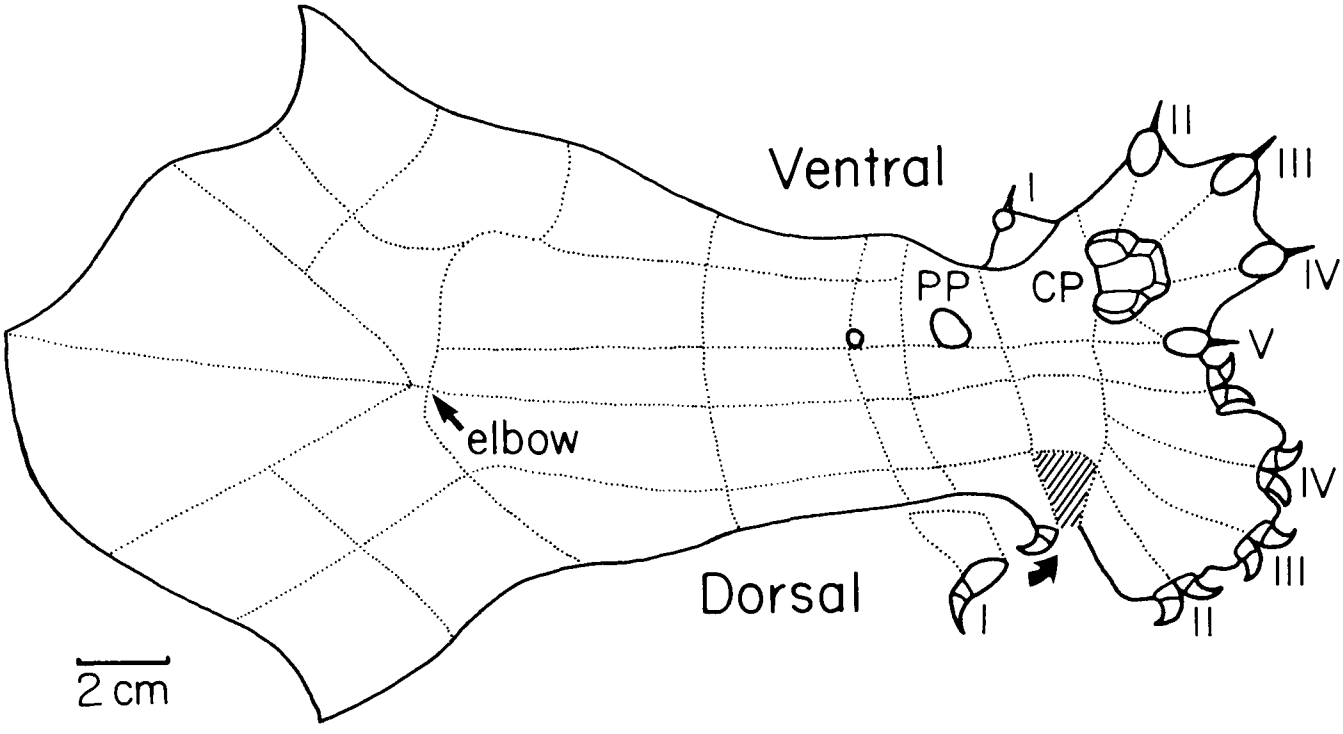

Fig. 1. Unfolded map of the surface of the cat's forelimb. Lines correspond to consistently identifiable morphological features; the same set of lines was traced on each subject before the experiment. PP, pisiform pad; CP, central pad. Roman numerals are digit numbers.

grid of reference lines (Fig. 1). This drawing was generated by removing the forelimb skin, with reference lines drawn on it, from the forelimb of one cat, and spreading it on a flat surface. Third, all the RFs collected in any given experiment were mapped by the same investigator. Fourth, the investigator who mapped RFs during an experiment was kept unaware about tendencies emerging in the data to prevent expectations from biasing the conduct of RF determinations.

During most experiments, penetrations were oriented approximately perpendicular to the cortical surface and, depending on the specific purpose of the experiment, were inserted into SI either singly or in closely spaced (75–150 μm apart) arrays of 16–25 penetrations. In one additional experiment, a linear array of 5 "tangential" penetrations were inserted deep into the bank of the coronal sulcus. Electrolytic lesions were made at the completion of penetrations to facilitate identification and reconstruction of the electrode tracks. At the termination of the experiments, subjects were anesthetized with Nembutal (35 mg/kg, IV) and perfused intracardially with saline followed by 10% formalin. The brains were imbedded in celloidin and cut serially; sections were stained with Cresyl fast violet. Cortical locations of the recording sites were determined from the reconstructions.

RESULTS

Demonstration of discrete column-shaped units in SI

Topographic boundaries detected with the minRF mapping method. Under general anesthesia, 16 microelectrode penetrations were inserted into the forelimb area of the postsigmoid gyrus. In the course of each penetration, the electrode was advanced in small steps from the pial surface to the white matter. Typically, the microelectrode travelled only 200–400 μm tangentially while advancing from the surface to the white matter (such penetrations are referred to as "near-radial"). Minimal RFs were mapped every 100–200 μm along the electrode track. In 3 of the 16 penetrations, all the minRFs mapped in a penetration occupied nearly the same position on the skin (for example, see Fig. 2A). The remaining 13 penetrations, however, were different—each contained 2 or 3 distinct sectors within which all minRFs were nearly identical. The different sectors of such penetrations were separated from one another by an abrupt shift of minRF to a clearly displaced position on the skin. Eight of the 13 penetrations contained 2 such sectors (an example is shown in Fig. 2B), and the other 5 penetrations contained 3 sectors (Fig. 2C). The transitions between sectors took place over 100–400 μm along the electrode track and were observed at all cortical depths below layer II. Above layer III, neural activity under general anesthesia was usually so weak that it was impossible to map minRFs.

In one experiment, 5 penetrations were directed nearly parallel to the cortical surface, down the medial bank of the coronal sulcus. Minimal RFs were mapped every 100 μm as the electrode advanced across radial cords of cells. In none of these 5 penetrations did the minRFs shift continuously or gradually as the electrode cut across the radial cords. Instead, each of the 5 penetrations contained several distinct sectors within which all minRFs were nearly identical; as was the case with the near-radial penetrations described

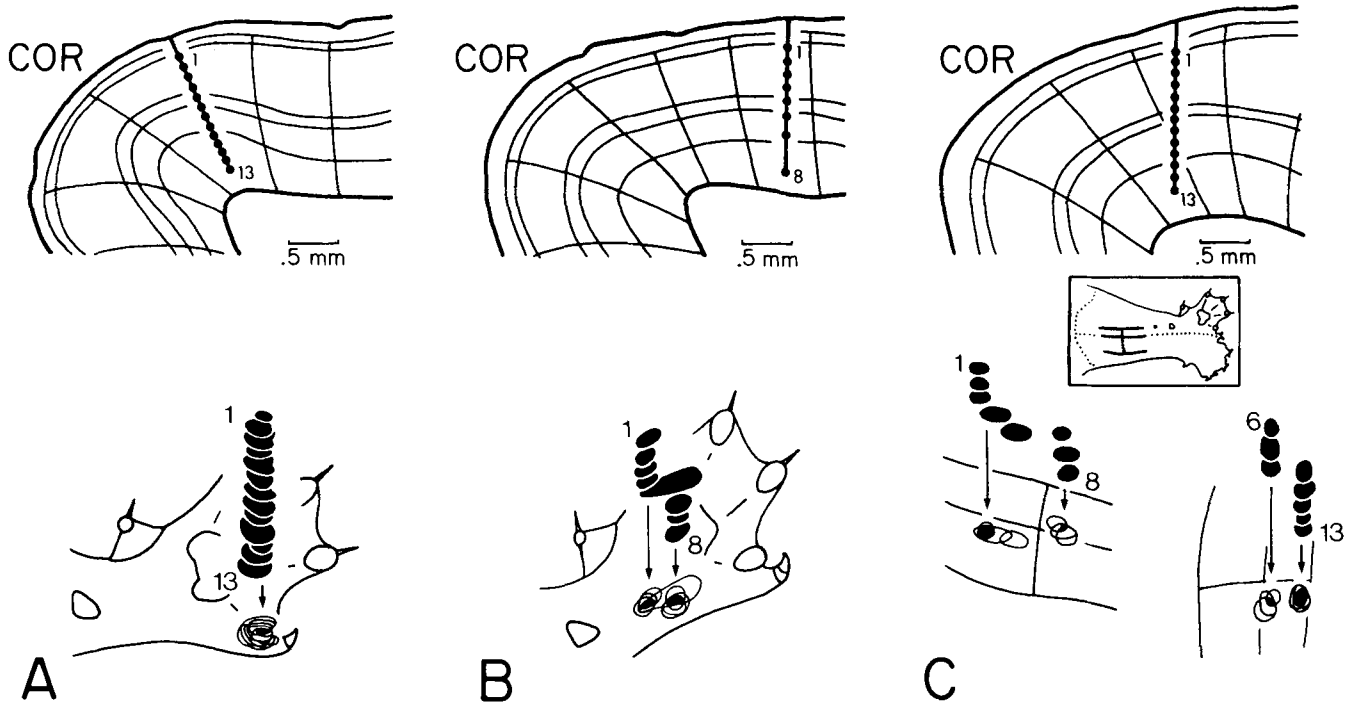

Fig. 2. Typical near-radial penetrations in which minRFs were mapped every 100–200 μm along the electrode track. In this and all following figures illustrating histological sections, orientations of radial cords of cells are indicated by thin lines and recording sites are indicated by circles. Minimal RFs are drawn in the order in which they were mapped in the penetration. (**A**) All minRFs occupy a single skin site for the entire penetration. (**B**) The penetration contains 2 distinct sectors; each sector contains nearly identical minRFs and adjacent sectors are separated one from another by an abrupt shift of minRF. (**C**) The penetration contains 3 distinct sectors separated by 2 abrupt shifts of minRF. The middle sector (minRFs 6–8) is shown twice to indicate the shift of minRF position occurring between the first and second sectors, and then between the second and third sectors.

previously, the sectors were separated from one another by an abrupt shift in minRF position (see, for example, Fig. 3). The transition from one sector to the next always occurred in less than 100 μm along the electrode track (because minRFs were taken 100 μm apart along the electrode track, it is impossible to be more precise about the length of the transition).

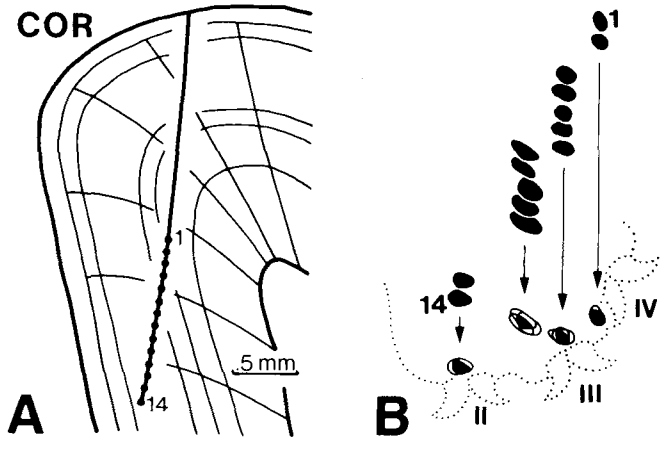

Fig. 3. Penetration in which minRFs were mapped every 100 μm along the electrode track as the electrode advanced approximately parallel to the cortical surface. (**A**) Histological reconstruction of the electrode track and the recording sites. (**B**) Minimal RFs mapped in the penetration. The penetration contains 4 distinct sectors, separated by 3 abrupt shifts of minRF position.

Thus penetrations that travelled approximately, but not exactly, parallel to radial cords of cells, as well as penetrations that cut across radial cords of cells, encountered topographic discontinuities in the cat SI. Since these abrupt shifts in minRF position were observed in the majority of near-radial penetrations (13 out of 16), and several of them were observed in each of the 5 tangential penetrations, such discontinuities appear to be a ubiquitous feature of the forelimb region of the SI. Furthermore, the finding that both near-radial and tangential penetrations contain sectors within which minRFs occupy essentially the same position on the skin suggests the presence in the SI of regions that are distinguished by their uniform minRF composition and by the absence of any consistent shift of minRFs within such regions.

One notable difference between the results of near-radial and tangential penetrations was observed. Specifically, transitions between neighboring internally homogeneous sectors of a penetration were significantly longer in near-radial penetrations than in tangential penetrations: typically 200–300 μm compared to less than 100 μm. This dependence of transition length on the angle of penetration suggests that the abrupt shifts of minRF position signal the crossing of topographic boundaries that are oriented perpendicular to the cortical surface and separate SI regions that possess nonoverlapping, prominently displaced minRFs.

What is the width of such topographic boundaries? In the near-radial penetrations, the length of transition between neighboring internally homogeneous sectors was 100–400 μm. Histological reconstruction of the electrode tracks showed that a 100–400 μm distance along the electrode

track corresponded to a 20–80 μm displacement in the plane parallel to the cortical surface. Thus the boundaries must be very sharp—no more than the width of one or, at most, 2 radial cords of cells, which are about 45 μm wide in the living brain. For example, the transition from one cortical region having one minRF to another region having a prominently displaced minRF may take place when crossing from one radial cord of cells to an adjacent one, or it may involve a "transitional" cell cord that lies at the border between these 2 regions and has a transitional minRF. Because in practice minRFs are mapped for populations of neurons residing within a cortical volume probably several tens of micrometers in diameter, the minRF mapping method cannot map a minRF of a single radial cord, but only a minRF that is an average of minRFs of several cords. As a result, crossing of a topographic boundary will always appear more gradual than it really is.

In summary, two major observations concerning the topographic organization of the forelimb region of the cat SI are described in this section. That is, this cortical territory contains (1) numerous topographic discontinuities, as well as (2) local cortical regions within which minRF position does not change with shifts in the position of the recording electrode. The most parsimonious explanation for these observations is that the forelimb region of the cat SI is organized as a mosaic of column-shaped, internally homogeneous (when studied with the minRF method) topographic units that are separated from each other by sharp boundaries. This possibility is evaluated experimentally in the subsequent sections of this work.

Topographic boundaries enclose discrete units. To corroborate the existence of the topographic units suggested by minRF data collected in single penetrations, we inserted arrays of closely spaced penetrations oriented approximately normal to the cortical surface into the forelimb region of SI of 4 deeply anesthetized cats. In each penetration 1 to 4 minRFs were mapped at 300 μm intervals along the electrode track. The depths of the recording sites were usually 0.5, 0.8, and 1.1 mm. The depths were chosen so as to include one minRF from layer IV. Following each of these 4 experiments, the electrode tracks were identified in histological sections and the locations of the recording sites were reconstructed in the plane of the cortical surface (more specifically, recording sites were projected along the radial lines onto the plane of the middle of layer 4).

Figure 4 shows the results of a representative experiment in which minRFs were mapped at 65 closely spaced cortical sites within a 0.8 × 0.8 mm region of SI of one subject. All cutaneous minRFs are plotted on a single drawing of the forelimb to reveal a most striking finding: 62 mapped cutaneous minRFs group to form 10 nonoverlapping clusters (Fig. 4B). From the 2-dimensional histological reconstruction of the electrode tracks and the locations of the recording sites (shown in Fig. 4C in the plane of cortical surface), it is clear that cortical recording sites that share the same minRF group together, whereas those that have different minRFs do not intermix. Especially evident is the clustering at just 2 skin sites (labeled "c" and "f" in Fig. 4) of minRFs obtained in the most thoroughly mapped cortical

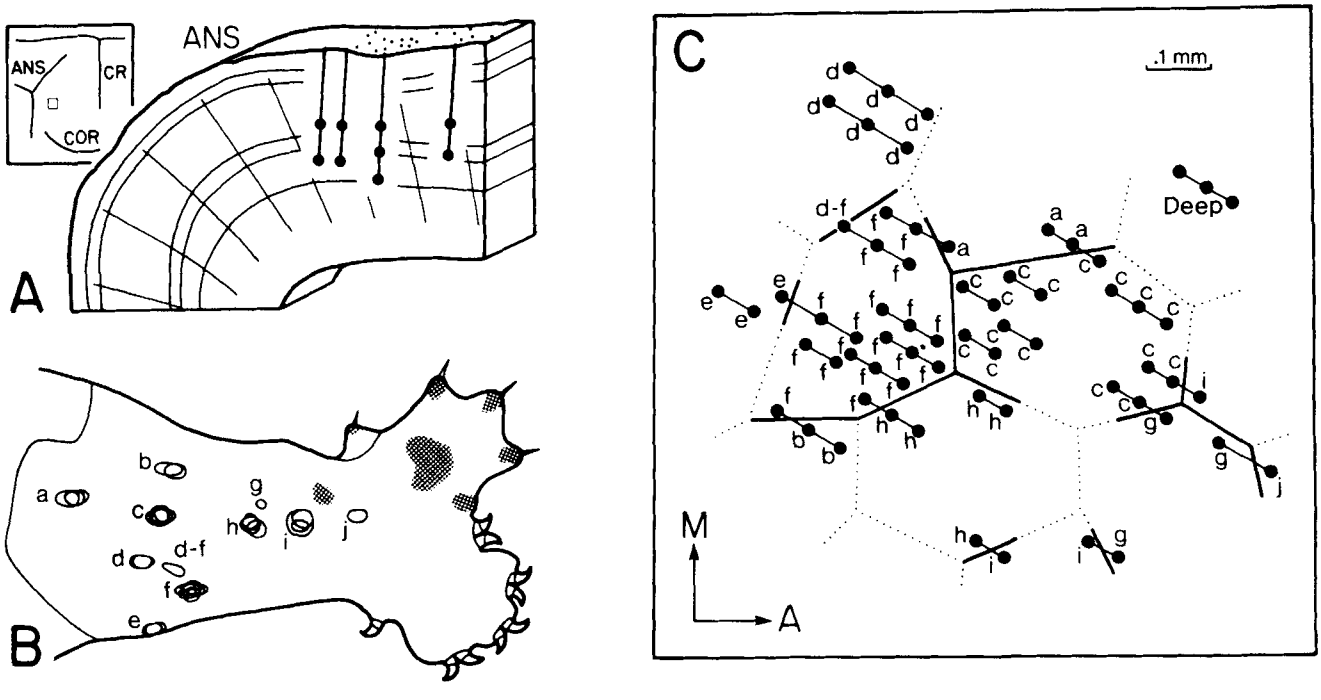

Fig. 4. Array of 25 closely spaced penetrations reveals discrete topographic units in SI. (**A**) Side view of cortex showing the location and orientation of the penetrations. Insert: surface view of somatosensory cortex. Area recorded from is enclosed in a rectangle. Labeled sulci: COR, coronal; ANS, ansate; CR, cruciate. (**B**) Outlines of the 62 minRFs drawn together to show that minRFs make up 10 discrete clusters, labeled a–j. One minRF, labeled d–f, was mapped in the transition zone where minRFs were shifting rapidly from site f to d. (**C**) Surface view of cortex showing positions of the recording sites (filled circles). Connected recording sites belong to the same penetration. Each recording site is labeled according to the discrete cluster to which its minRF belongs. Solid lines indicate cortical locations where minRF shifts abruptly; dotted lines indicate cortical locations where abrupt shift of minRF is likely to be found assuming that all topographic units in the mapped cortical region have *similar* dimensions.

region. The data offer no evidence of any gradual, continuous shift of minRFs on the skin as the cortical position of the recording electrode is shifted.

An abrupt shift of minRF, signalling the crossing of a topographic boundary, occurred in 11 penetrations. In addition, at some cortical locations an abrupt shift of minRF (and, therefore, a topographic boundary) was inferred from the presence in neighboring penetrations of adjacent recording sites with nonoverlapping minRFs. When these topographic boundaries are indicated as solid lines (as they are in Fig. 4C), 2 discrete cortical regions can be discerned. Because within each region, all recording sites have nearly identical minRFs, both regions appear to be topographic entities, or units. Although less detailed, the minRF data from the cortical territories surrounding the 2 identified topographic units are completely consistent with the idea that similar units exist throughout the entire studied cortical field (see boundaries indicated by solid and dotted lines in Fig. 4C).

What is the size and shape of the 2 topographic units identified in this experiment? According to the reconstruction of boundaries shown in Figure 4C, each unit is bordered by 6 different units. If, as a first approximation, the boundaries separating the 2 adjacent units are assumed to be straight, then both units take the shape of irregular, elongated hexagons. In the living brain, the shortest and longest distances between opposite sides of the 2 units are 250 and 350 μm.

Another experiment in which a grid of closely spaced, near-radial penetrations was made is illustrated in Figure 5. In this case, 51 minRFs were mapped in the 0.6 × 0.9 mm cortical region that received its principal input from digits 4 and 5 (Fig. 5B). It is of interest to note that in contrast to the experiment illustrated in Figure 4, some of the minRFs mapped in this experiment had larger than usual sizes and showed greater than usual variability in their position. These large minRFs were mapped at cortical sites where the recorded neuroelectrical activity was dominated by one or 2 single units with action potentials much larger than those of the rest of the recorded neuronal population. Although we always tried to avoid such recordings (by moving the location of the recording site slightly; see Methods), this was not always possible in this particular experiment because the microelectrode used during this experiment had a very strong tendency to record spikes of one or 2 single units at most recording loci. This example illustrates the sensitivity of the minRF mapping method to the properties of the recording electrodes. Nevertheless, it is evident that the minRFs mapped in this experiment group about 6 discrete skin loci, labeled "a" to "f" in the

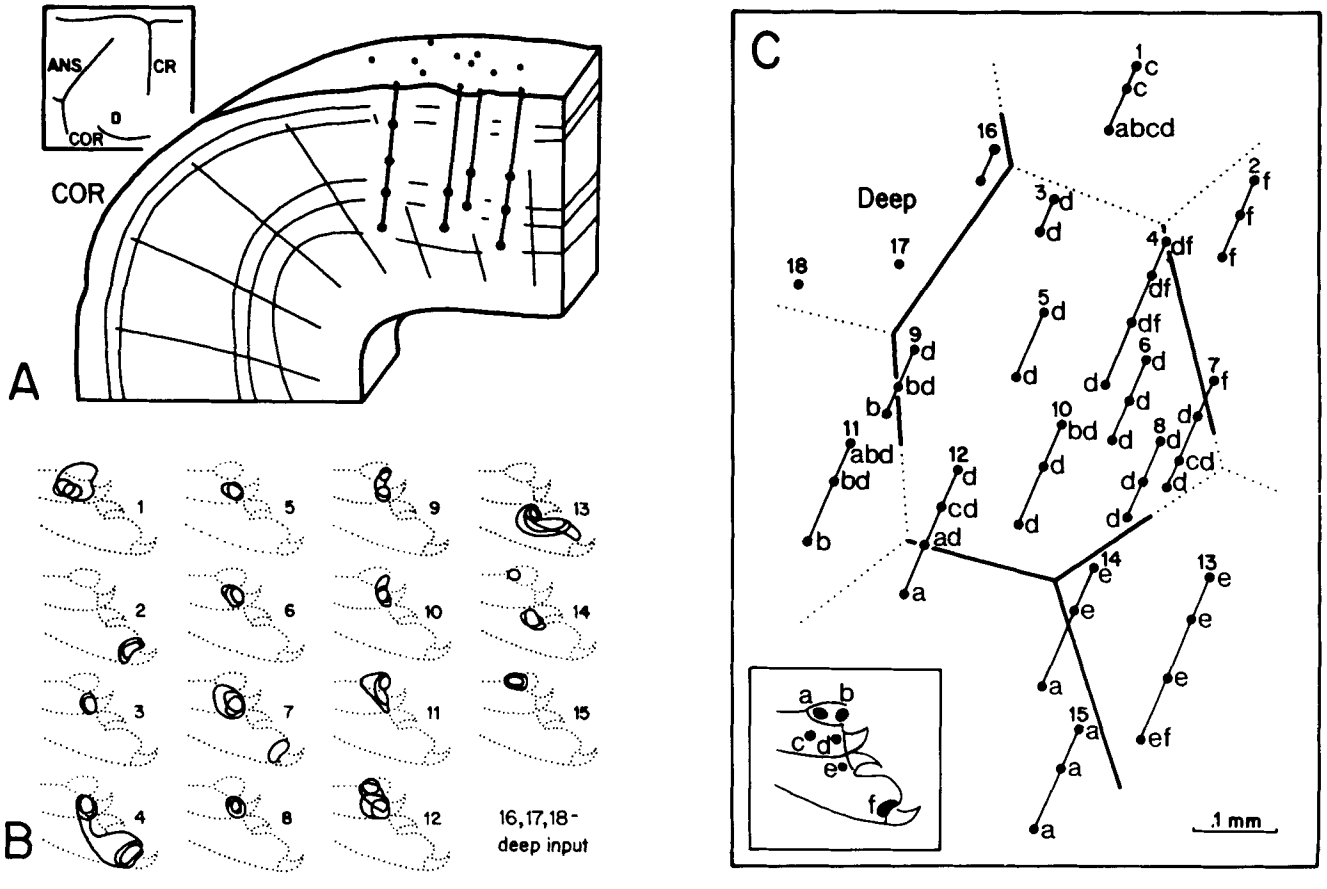

Fig. 5. Discrete topographic unit is revealed in an array of 18 closely spaced penetrations. Format is similar to Figure 4. (**A**) Location and orientation of the penetrations. Inset shows location of studied cortical region. (**B**) Minimal RFs mapped in all 18 penetrations. Outlines of all minRFs mapped in a given penetration are drawn together. (**C**) Surface view of the cortex showing positions of the recording sites. Each penetration is identified by the same number as in part B, and each recording site is labeled according to the discrete skin loci (see inset) included in its minRF. Insert: minRFs are clustered about 6 skin loci, labeled a–f.

inset of Figure 5C. At 4 recording sites, cutaneous stimuli were not effective; the most effective peripheral stimulus at these 4 sites was the extension of digit 5.

Two-dimensional histological reconstruction of the electrode tracks and the recording sites is shown in Figure 5C. The reconstruction provides no evidence that, as the electrode was moved across the cortex, minRFs shifted in a gradual and continuous manner across the skin. Instead, 6 cortical regions can be distinguished in Figure 5C, and within each region all recording sites share the same skin locus in their minRFs. Thus recording sites whose minRFs do not overlap are located in different cortical regions. The most parsimonious interpretation of these data is that they reveal 6 distinct cortical regions, each of which receives its strongest input from a different skin locus on the digits (indicated as "a" to "f" in Fig. 5). It is also of interest in this regard that the 4 recording sites that receive deep mechanoreceptor input also group together and appear to define a separate, seventh cortical region. That the transition from one of these regions to another is abrupt is suggested by the demonstration of an abrupt shift of minRF position on the skin at a number of cortical locations. Such abrupt shifts were detected within 5 of the penetrations shown in Figure 5, as well as between several adjacent cortical sites sampled in different penetrations.

If the above interpretation of the minRF data of the experiment shown in Figure 5 is correct, it suggests an arrangement of 7 topographic units in the studied cortical field: the unit in the center of the field is bordered by 6 other units, one of which receives deep input. In Figure 5C the linear boundaries assigned to the inferred topographic units are shown by solid lines at the locations where they are demonstrated directly, and by dotted lines at locations where they were not demonstrated directly due to a low density of penetrations, but can be expected assuming that all topographic units in the mapped cortical region have similar dimensions. According to the reconstruction of the topographic units shown in Figure 5C, the central unit has the shape of an irregular, elongated hexagon with shortest and longest distances between opposite sides of 350 and 460 μm.

The two other experiments of this study that used arrays of near-radial penetrations yielded results completely consistent with those described in Figures 4 and 5. In one additional experiment, a different mapping strategy was used: a linear array of 5 penetrations was inserted deep into the medial bank of the coronal sulcus. As the electrode advanced across this region's radial cell cords, minRFs were mapped at 100 μm intervals. The results of this experiment are shown in Figure 6. Minimal RFs were mapped at 59 cortical recording sites, 4 of which received deep input from digit 3. The remaining 55 recording sites received cutaneous input from the dorsal surface of digits 2, 3, or 4. Despite the very different angle of penetration, the minRF data collected in this array of surface-parallel penetrations resemble closely the minRF data collected in the arrays of near-radial penetrations. First, when plotted on a single drawing of the dorsal surface of the paw, the 55 minRFs form 8 discrete clusters (Fig. 6B). Second, according to the 2-dimensional histological reconstruction of the penetrations, recording sites with identical or very similar minRFs group together in the cortex, segregated from groups of recording sites with different minRFs (Fig. 6C). Third, all 5 penetrations cross sharp topographic boundaries, as evidenced by abrupt shifts of minRF position, and these boundaries subdivide the penetrations into distinct sectors within which all minRFs are nearly identical. Taken together, these observations suggest the presence in the studied cortical territory of a mosaic of 9 discrete topographic units. Each unit is distinguished by the uniformity of minRFs within it and by the abrupt shift of minRF at its border with neighboring units.

Because the minRFs collected in the experiment described above were mapped when the electrode tip was deep in the cortex of the medial wall of the coronal gyrus, the relative locations of recording sites from different penetra-

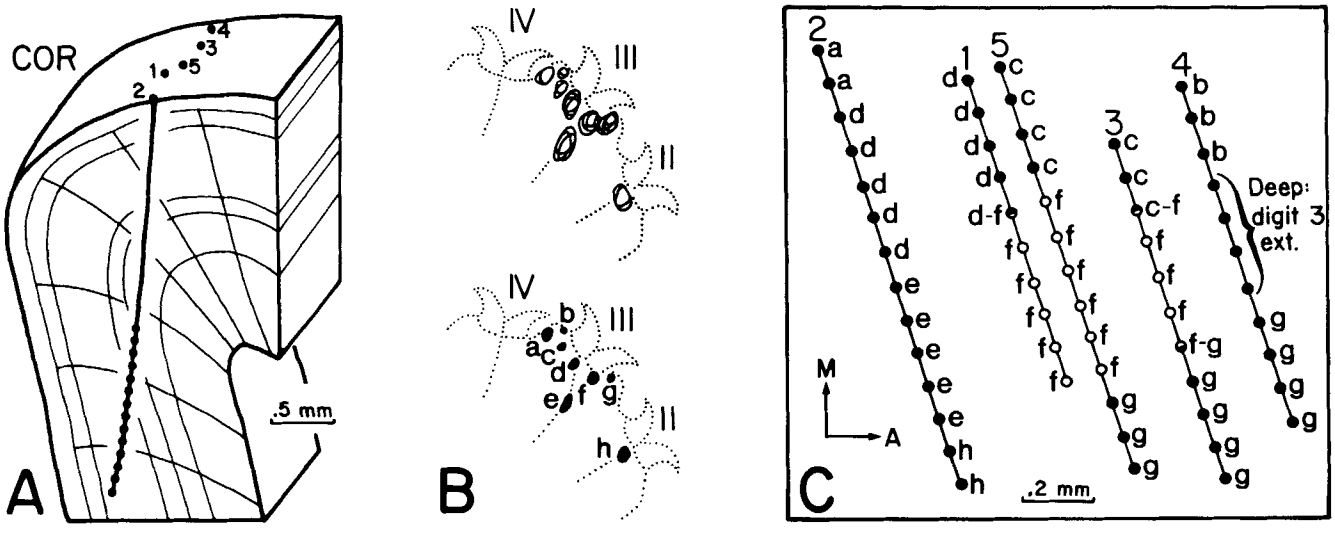

Fig. 6. Discrete topographic units are revealed in an array of 5 penetrations aligned perpendicular to the orientation of radial cell cords. (**A**) Minimal RFs were mapped every 100 μm as the electrode advanced down the bank of the coronal (COR) sulcus. Penetration 2, the most posterior one (also illustrated in Fig. 3), is shown in its entirety. (**B**) Top: the 55 cutaneous minRFs form 8 discrete clusters. Bottom: the site of overlap of each cluster is labeled, a–h. Roman numerals are digit numbers. (C) Reconstruction of the 5 parallel penetrations as seen in the plane tangential to the cortical surface. Each recording site (circle) is labeled according to the discrete cluster to which its minRF belongs.

tions could not be specified with the precision possible for near-radial penetrations of the crown of the postsigmoid gyrus. For this reason, the reconstruction shown in Figure 6C represents our best estimate of the relative positions of the penetrations. In view of the uncertainty about relative locations of the recording sites, however, no attempt was made to draw the boundaries of the topographic units, or to evaluate their size and shape.

To date, 6 topographic units have been mapped at a resolution sufficient to reveal their shape and size. Each of these 6 topographic units had a slightly elongated convex shape and was found to be bordered by 6 surrounding units. Size varied among the 6 units in a systematic way depending on the position of the unit's minRF on the forelimb: 2 units with minRFs on the proximal forearm (Fig. 4) had an average width of 300 μm, one unit with minRF on the distal forearm had an average width of 330 μm, 2 units with minRFs on the wrist had an average width of 370 μm, and one unit with minRF on digit 5 (Fig. 5) had an average width of 400 μm. Thus it appears that units with minRFs on more distal parts of the forelimb are larger than units with minRFs on more proximal parts of the forelimb.

Internal composition of topographic units

When studied with the minRF mapping method, the topographic units identified in the preceding section appear as internally homogeneous cortical columns, with nearly identical minRFs mapped at all locations sampled within a given unit. This makes the minRF approach a very convenient physiological method for demonstrating topographic boundaries and for mapping the shape of the topographic units. However, because the method is designed to reveal only the strongest peripheral input to the entire recorded neuronal population, important details of within-unit organization undoubtedly escape demonstration. For this reason, we investigated the internal organization of topographic units within the forelimb region of the cat SI using the maxRF mapping method. This alternative RF mapping approach identifies not only the skin area providing the strongest input to an individual recorded neuron, but also reveals those skin areas providing less than maximal input to that neuron. The maxRFs analyzed here were collected in the course of 16 near-radial microelectrode penetrations in which the spike discharge activity of 10 or more (up to 25) single neurons was isolated, and the maxRF of each neuron was accurately mapped. Representative observations are shown in Figures 7 and 8.

Maximal RF data reflect the existence of SI topographic units. The most pronounced feature of the maxRFs collected in any near-radial penetration of SI is the great diversity in the size and shape of the individual maxRFs. This is readily apparent in the data shown in

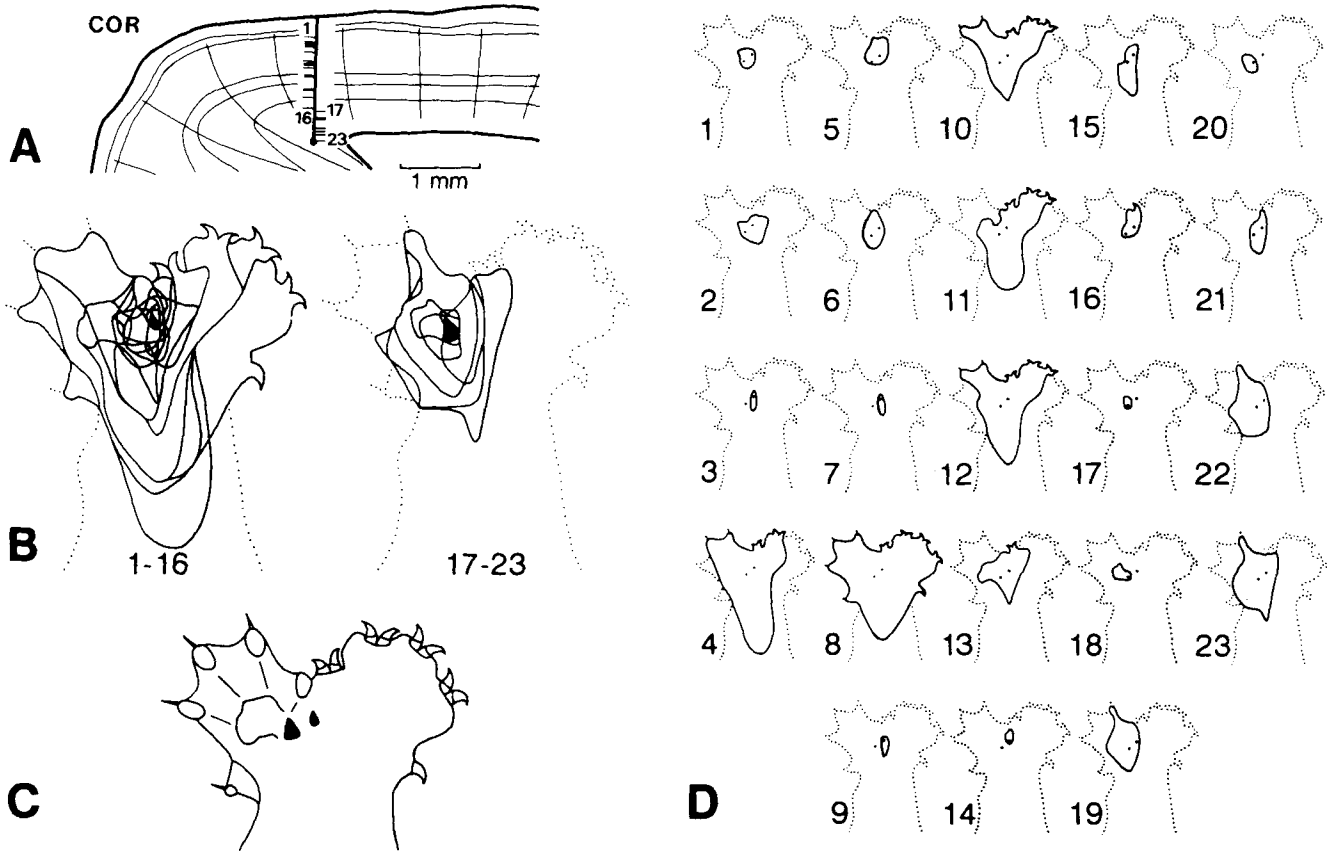

Fig. 7. Sequence of single neuron maxRFs mapped in a penetration that crossed a topographic boundary. (**A**) Histological reconstruction of the penetration. Sites at which single neurons were isolated are indicated by dashes. COR, coronal sulcus. (**B**) Superimposed outlines of maxRFs collected in two sectors of the penetration. Filled black areas are skin regions shared by all the maxRFs in a sector. (**C**) Relative positions of the areas shared by maxRFs of neurons 1–16 and 17–23. (**D**) The 2 sites of maxRF overlap (small dots) are shown relative to all 23 maxRFs.

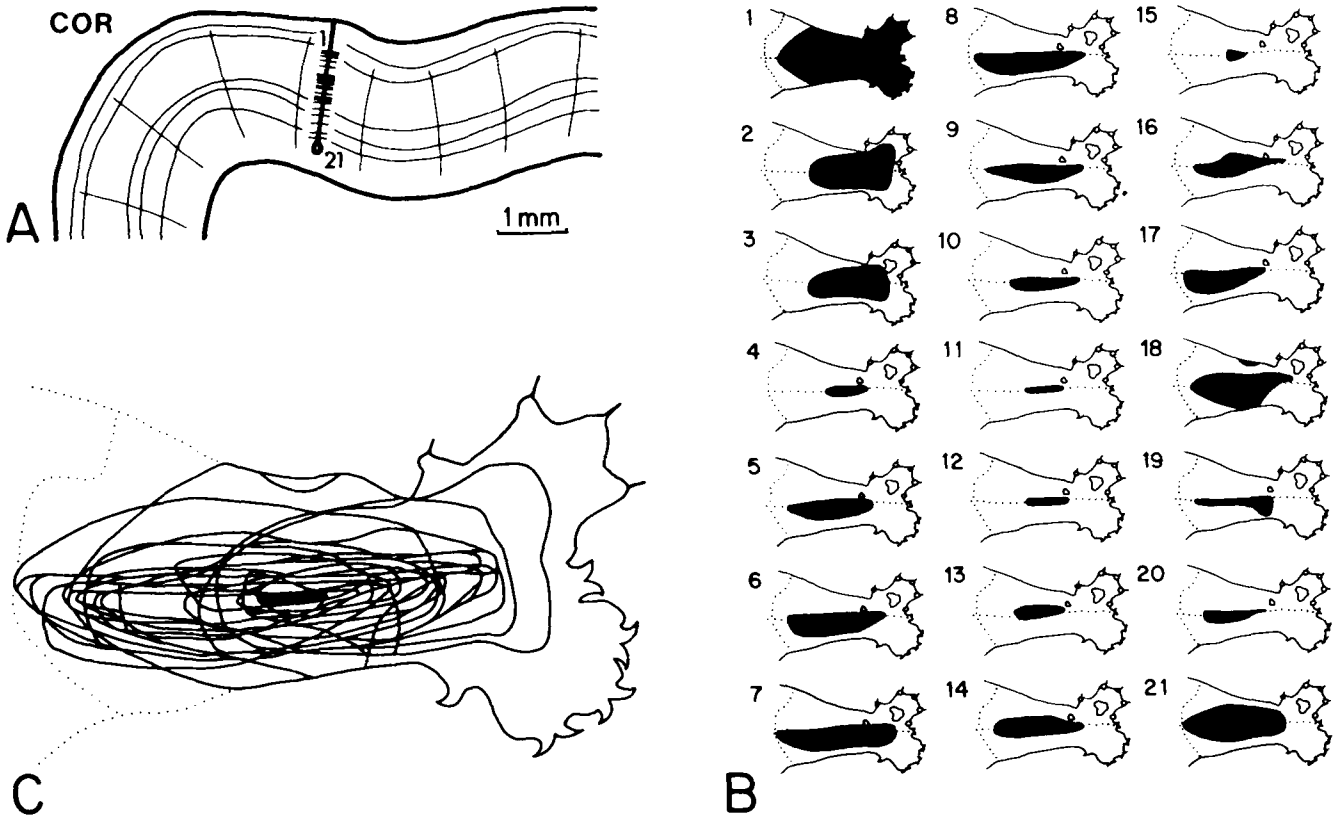

Fig. 8. Sequence of single neuron maxRFs from a penetration that remained within a single topographic unit. (**A**) Histological reconstruction of the penetration. COR, coronal sulcus. Sites at which single neurons were isolated are indicated by dashes. (**B**) Maximal RFs of 21 single neurons. (**C**) Superimposed outlines of all 21 maxRFs. Blackened area is the skin site included in each of the maxRFs.

Figures 7 and 8. The variability is not random, however, for a subtle order can be discerned in the data; its character becomes apparent when it is realized that there is a restricted skin area common to all the maxRFs sampled serially during much or all of a near-radial penetration. In an earlier work (Favorov et al., '87), we showed that within a sector of a near-radial penetration, which is distinguished by near identity of its minRFs, all isolated single neurons include in their maxRFs the skin area covered by the minRF mapped in that sector. Furthermore, the skin area covered by the minRF is the only skin area invariably included in the maxRFs of the single neurons isolated in such a sector. Thus just as was the case for minRF penetrations, during maxRF penetrations sectors also can be identified within which all the maxRFs include the same small skin area. For example, no single skin area is common to all the maxRFs mapped in the course of the penetration illustrated in Figure 7. However, two contiguous sectors can be identified within this penetration such that the maxRFs of all the neurons in a given sector include one skin site in common. Furthermore, the maxRFs of the neurons in the adjacent sectors define common skin loci that are not only nonoverlapping, but even noncontiguous and prominently separated from each other. More specifically, the maxRFs of the first 16 neurons isolated in the penetration share in common one small skin site on the ulnar edge of the forepaw (Fig. 7B). Neuron 17, however, does not include this skin site in its maxRF. Instead, neurons 17 to 23 share in common a different skin site, a small region at the base of the central pad (Fig. 7C). The reason for the absence of any skin area common to the maxRFs of all the neurons in this penetration is that maxRFs of neurons 3, 7, 9, and 14 do not overlap maxRFs of neurons 17, 18, and 20 (Fig. 7D).

The absence of any skin locus common to maxRFs of all the neurons isolated in the penetration shown in Figure 7 suggests that this penetration sampled neurons from more than one topographic unit. The presence in this penetration of 2 sectors, such that within each sector all maxRFs share in common a single skin site, further suggests that the penetration was limited to 2 topographic units. At what point along the track did the electrode tip cross the boundary between the first topographic unit and the second? Since the maxRF of neuron 14 does not include the skin site common to the maxRFs of neurons 17–23, neuron 14 must belong to the first topographic unit. Further, since the maxRF of neuron 17 does not include the skin site common to the maxRFs of neurons 1–16, neuron 17 must belong to the second topographic unit. Since the maxRFs of neurons 15 and 16 include both common skin sites, these 2 neurons cannot be assigned exclusively to either unit. Thus the crossing from the first topographic unit to the second must have occurred at some point between the locations of neurons 14 and 17. The distance along the electrode track between neurons 14 and 17 is 240 μm, but in the plane of the cortical surface it is much smaller—only 60 μm (measured on the histological section shown in Fig. 7A), approximately the same length as the transition between neighbor-

ing topographic units when measured using the minRF method.

Overall, of the 16 penetrations in which maxRFs were mapped, 7 penetrations were of the type shown in Figure 7, in that these penetrations had to be subdivided into 2 sectors in order for all the maxRFs mapped in a sector to include one skin site in common. In 7 other penetrations, all the maxRFs mapped in a penetration shared a common skin site, suggesting that those penetrations remained within a single topographic unit for their entire length. An example of one such penetration is provided in Figure 8. The remaining 2 penetrations of this series had to be subdivided into 3 sectors for all maxRFs in a sector to have a common skin site. These 2 penetrations apparently travelled through 3 different topographic units. In the 9 penetrations that had to be subdivided into 2 or 3 sectors, 47% of neurons in one sector of the penetration did not include in their maxRFs the skin locus common to maxRFs of all the neurons isolated in the adjacent sector.

Relationship between RF similarity and cortical distance offers insights into the internal organization of SI topographic units. As pointed out in this and previous publications (Iwamura et al., '85; Favorov et al., '87; Favorov and Whitsel, '88a,b), large variations in size and shape are characteristic of the maxRF data collected in near-radial penetrations of the SI of unanesthetized subjects. Accordingly, one of the questions addressed in the present study was, Can analysis of maxRF variability provide any information about the inner structure of topographic units? A particular approach chosen in the present study was to select quantitative indices of the similarity between pairs of maxRFs and to construct plots showing how these indices change with increasing distance between the recording sites at which the compared maxRFs were mapped. The analysis was applied to maxRFs of 260 single neurons, mapped in the 16 penetrations described above. After identifying topographic boundaries according to the criterion given in the preceding section, each neuron was paired with all other neurons isolated in the same penetration in the same topographic unit. A total of 1,111 neuronal pairs were formed, such that both members of the pair were isolated in the same topographic unit. For each pair, 2 measures of RF similarity were computed: the degree of maxRF overlap and ratio of maxRF sizes (see Fig. 9A for definition of these 2 measures). In order to highlight the magnitude of maxRF variability, among even very closely located neurons, the values of the 2 measures are plotted for all 1,111 pairs of neurons, as a function of the distance along the electrode track separating the pair of neurons (Fig. 9B).

For the purpose of uncovering any dependence of RF similarity on cortical distance, pairs of neurons were sorted into bins based on the distance along the electrode track between the neurons. For the pairs of neurons in each distance bin, the average degree of RF overlap and average ratio of RF sizes were computed, and these indices are shown graphically in Figure 9C. The plot shows that RF similarity is, on average, higher for pairs of neurons located next to one another than it is for pairs of more widely separated neurons. The relationship is not linear, however, since most of the decline in RF similarity with increasing distance takes place at separations less than 200 μm. At separations larger than 200 μm, RF similarity within an SI topographic unit is essentially independent of the distance (along the electrode track) between neurons.

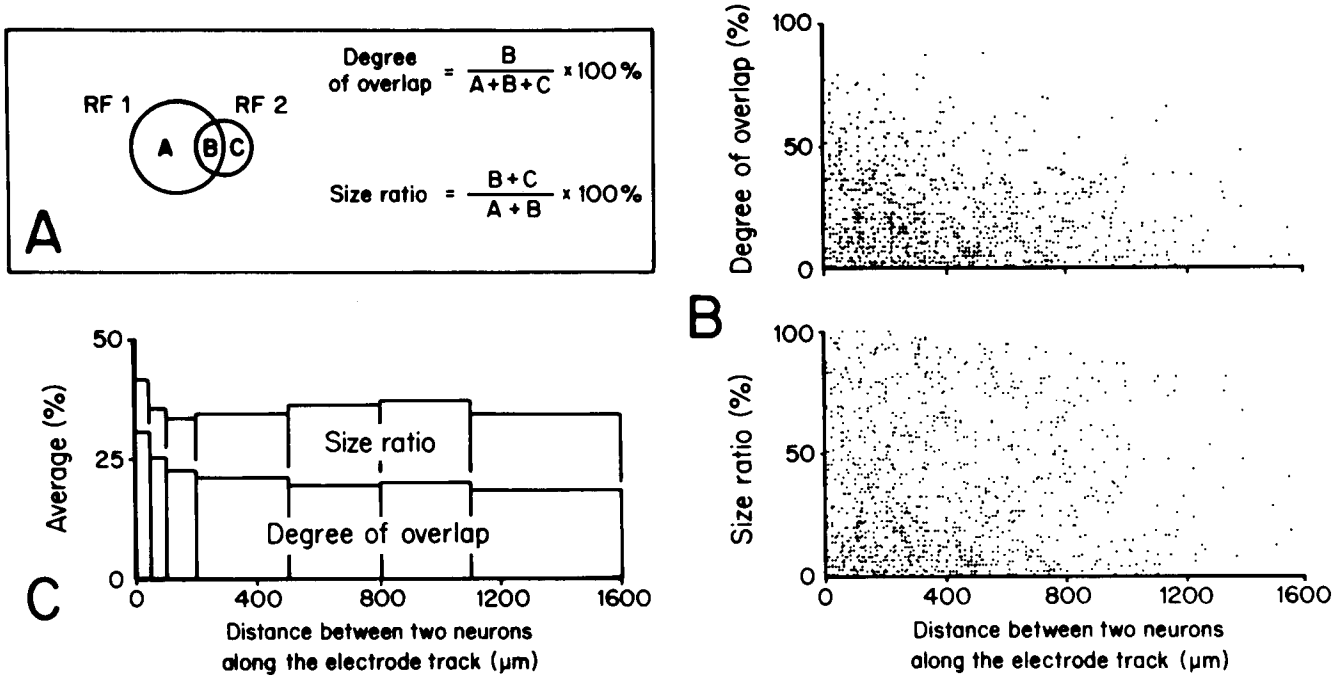

Fig. 9. Receptive field similarity vs. distance between neurons along the electrode track. Pairs of maxRFs were formed only for neurons isolated in the same penetration and in the same topographic unit. (**A**) Two measures of RF similarity: degree of overlap and ratio of sizes (smaller RF/larger RF) of a pair of maxRFs. (**B**) Degree of overlap and size ratio for all pairs of maxRFs (n = 1,111) plotted against the distance separating members of a pair. (**C**) Superimposed histograms showing average degree of maxRF overlap and average size ratio as functions of cortical distance.

The results shown in Figure 9 reveal aspects of the internal organization of topographic units that are directly relatable to the underlying cellular architecture of the SI. A crucial element in our recognition of this relationship was the finding that a 200 μm advance along the near-radial electrode track resulted, on average, in a 40 μm advance in the plane of the cortical surface. From this perspective, therefore, most of the decline in RF similarity occurs when the electrode is advanced just far enough to cross one radial cord of cells (their diameter in the living brain is approximately 45 μm). This observation brings to attention the fact that SI cortex contains 2 types of neurons that distribute afferent input radially within the confines of individual radial cords of cells (Jones, '75, '81). They are double bouquet cells of layer 2 and spiny stellate cells of layer 4, or according to the classification of Jones ('75), cell types 3 and 7; both types of cells have fields of axonal termination that are restricted in the tangential plane (diameter frequently less than 50 μm) and extend radially through most cortical layers. Such an organization of the axonal fields is likely to impose heightened uniformity on the RF characteristics of the neurons residing within the same radial cord. As a result, pairs of neurons located in the same radial cord of cells can be expected to have maxRFs more similar than those of pairs of neurons located in different cell cords (Favorov and Whitsel, '88b). The data shown in Figure 9C are entirely consistent with this expectation. That is, neurons separated by 50 μm or less along the electrode track (these neuron pairs comprise the first bin of the histogram) have the greatest likelihood of occupying the same radial cord of cells. Neurons separated by progressively greater distances (over the range between 50–200 μm) have a progressively declining likelihood of occupying the same radial cord. This fact, when taken together with the assumption that neurons within the same radial cord have the most similar maxRFs, leads to the expectation—confirmed by the histogram in Figure 9C—that as the distance between neuron pairs increases, average RF similarity should decline.

If one accepts the above explanation for the observed decline of RF similarity in the first 3 bins of the histogram in Figure 9C, two additional suggestions can be drawn from the plots in Figure 9. First, Figure 9B suggests that the maxRFs of even neurons located within the same radial cord of cells are not identical: this suggestion derives from the fact that the leftmost part of the degree of RF overlap scatter plot does not contain any data points at or near the 100% level. Second, in traversing a topographic unit tangentially—and moving from one radial cord to the next—there are large variations in maxRF size and shape (Fig. 9B), but it appears that there is only a very small, if any, overall shift in maxRF position across a topographic unit. This is shown in Figure 9C by only a very slight decline in average degree of RF overlap with increasing distance above 200 μm, whereas average RF size ratio appears not to change at all.

The maxRFs of neurons located on opposite sides of a topographic boundary occupy partially shifted skin territories. Considering that minRFs mapped on the opposite sides of a topographic boundary occupy prominently displaced skin loci, it is reasonable to expect that the maxRFs of the neuron populations lying on opposite sides of a topographic boundary also occupy (on average) different positions on the skin. To evaluate this prediction, we applied the analysis of maxRF similarity described in the preceding section to the maxRF data collected in single penetrations on the opposite sides of topographic boundaries. As indicated previously, 9 penetrations of this study crossed either one or 2 topographic boundaries. In these penetrations pairs were formed between neurons isolated on opposite sides of the boundary separating adjacent topographic units. For each pair of neurons, degree of overlap of their maxRFs and maxRF size ratio were computed.

Figure 10 compares the maxRF data collected within topographic units with the maxRF data collected on opposite sides of topographic boundaries. According to Figure 10A, the distribution of RF size ratios for neuron pairs taken across a topographic boundary is very similar to the distribution for pairs taken within a unit. This indicates that neurons on both sides of a unit boundary have the same assortments of maxRF sizes. In contrast, the distribution of computed values of RF overlap for neuron pairs sampled on opposite sides of a topographic boundary is shifted to the left relative to the distribution of values of RF overlap for neuron pairs sampled within a unit (Fig. 10B). As a result, average degree of RF overlap is much smaller for neuron pairs located on opposite sides of a topographic boundary than it is for neuron pairs located within the same unit—11% versus 21%. Most prominently, maxRFs of 30% of the pairs of neurons lying on opposite sides of a unit boundary do not overlap at all, nor are they contiguous (see first bin of bottom panel of Fig. 10B). Of course, all pairs of neurons within a given unit possess overlapping maxRFs (Fig. 10B, top panel).

Finally, since degree of RF overlap is determined by a combination of two factors—the relative sizes of the compared maxRFs, and their relative positions on the skin—and since neurons have the same assortment of maxRF sizes whether they are located within the same topographic unit or on opposite sides of a unit boundary, their difference in the degree of RF overlap must be due to the fact that the maxRFs of neurons located on opposite sides of a unit boundary are displaced (on average) on the skin relative to each other. Moreover, the displacement must take place at the point of the boundary crossing, because no group displacements of maxRFs are observed among cords of cells lying within a topographic unit.

DISCUSSION

Since the earliest studies of the SI cortex with evoked potential mapping methods (Marshall et al., '37), it has been viewed as organized in a continuous, essentially somatotopic manner. A number of prominent topographic discontinuities were recognized even in these earliest studies, but their existence did not detract from the idea that the global plan of SI topographic organization was somatopic. In later higher resolution studies, additional topographical discontinuities were found (for reviews see Kaas et al., '81; Merzenich et al., '81). Topographic discontinuities were also found at the interface between cortical columns receiving input from different mechanoreceptor classes (for example, at the borders between "deep" and "skin" columns, and sometimes at the boundaries between columns distinguishable on the basis of neuronal adaptation properties; Dykes and Gabor, '81). Despite the presence of such topographic discontinuities, however, it has remained generally accepted that the organization within large blocks of SI is somatotopic and continuous; i.e., within these large sectors of the SI, neighboring columns cannot

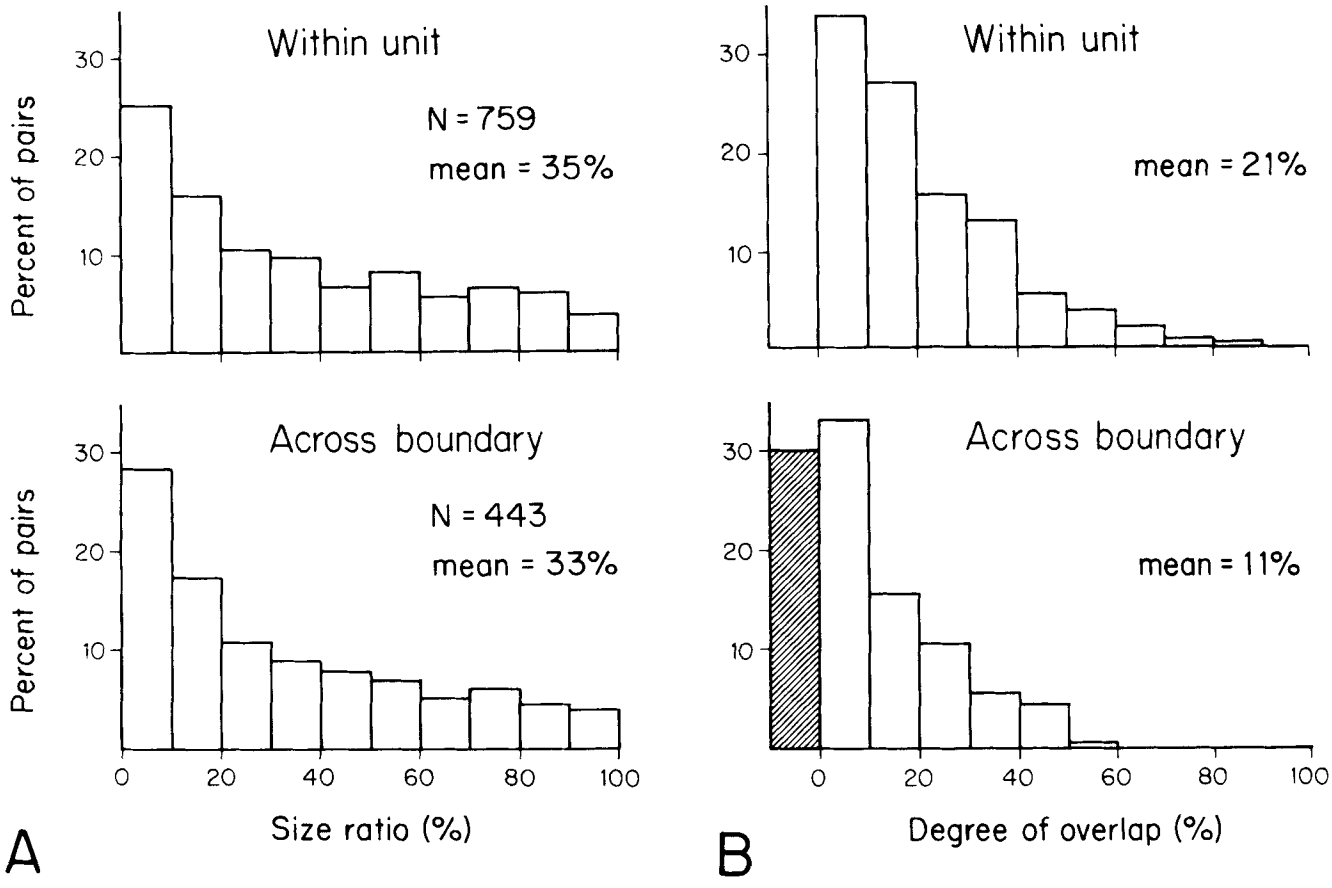

Fig. 10. Comparison of pairs of maxRFs mapped within the same topographic unit versus pairs of maxRFs mapped on the opposite sides of a boundary between two topographic units. (**A**) The distributions of size ratios of maxRFs. (**B**) The distributions of degrees of maxRF overlap. Note that the shaded bar in the bottom plot represents pairs of nonoverlapping, noncontiguous maxRFs.

be unambiguously distinguished on the basis of the place on the body that provides their input (see, for example, Dykes and Ruest, '86). Mountcastle's original papers ('57; Powell and Mountcastle, '59) on SI columnar organization are consistent with this view. Although Powell and Mountcastle reported some evidence, obtained in anteroposterior penetrations of the monkey's area 3b, suggestive of discrete place-defined columns, they also noted that in penetrations that advanced in the mediolateral dimension of SI RFs shifted "very rapidly and continuously" (p. 153). Similarly, in his 1957 paper on the cat SI, Mountcastle wrote that "when slanting penetrations . . . are made, the receptive fields of neurons successively encountered shift gradually, in conformity with the surface pattern of representation directly above the successive positions of the electrode tip in the depths" (p. 419).

Responding to the existing consensus that SI cortical columns are place-specific but not place-defined, Mountcastle emphasized in a review chapter in "The Mindful Brain" ('78) that the columnar hypothesis does not require that the lateral borders of cortical columns be definable on the basis of RF position: "the columnar organization is compatible with partially shifted overlap in the representation of the body form" (p. 20). The basis for this conclusion is that the "cortical column is established by virtue of anatomical connections—its specific afferent input and its vertically oriented intrinsic connectivity—but also in a dynamic manner by a strong pericolumnar inhibition" (p. 32). Therefore, pericolumnar or lateral inhibition ensures the functional isolation of active SI columns from their neighbors; as a result, cortical activation occurs in the form of sharply delineated column-shaped aggregates ("macrocolumns"; Mountcastle, '78) even at locations where the afferent connections to neighboring cortical sectors convey information arising from only partially shifted, extensively overlapping skin regions.

The results of the present study conflict with the widely held idea that the representation of the body surface in large regions of SI is organized in a continuous manner. Instead, the results of every experiment are consistent with the presence of a modular, honeycomblike topographic organization; a type of organization that has also been proposed for area 1 of the *Macaca fascicularis* monkey (Favorov and Whitsel, '88a). Specifically, we interpret our experiments to have identified discrete column-shaped neuronal aggregates in cat SI—topographic units—300–400 μm in diameter. These neuronal aggregates can be identified with either minRF or maxRF methods: (1) because nearly identical minRFs are mapped within each aggregate, and (2) because maxRFs of all the neurons comprising each aggregate have a common skin area. To underscore the idea that these columns were discrete and nonoverlapping, they were originally given the name "segregates" (Favorov et al., '87; Favorov and Whitsel, '88a).

Diversity of single neuron RFs within a segregate. The maxRFs of single neurons located in the same segregate vary greatly in size and configuration; it is conceivable that no 2 neurons in a segregate have exactly the same maxRFs—so much so that there is only one very small skin site that is common to the maxRFs of all neurons in the segregate. As was shown in an earlier work (Favorov et al., '87), this shared skin site is also the skin site covered by the minRFs mapped within that same segregate. Thus whereas maxRF data collected from single neurons indicate that the peripheral input to the neurons comprising a segregate is spatially extensive and highly varied, they also indicate that the variability is not random but is organized with respect to the skin locus common to all maxRFs. The organization is perhaps best described in the following way: the maxRF of each neuron in a segregate includes the common skin locus and, in addition, it extends for variable distances outward in all directions from that locus. Therefore, the maxRFs within a segregate differ from one another in how much they extend in each and every direction from the common skin locus. Because of its central importance to segregate organization, the common skin locus of a segregate was given a special name, "segregate RF center" (Favorov and Whitsel, '88a).

The unitary nature of the segregate. The original view of a place-defined cortical column was that it should be composed of neurons with very similar RFs (Mountcastle, '57; Powell and Mountcastle, '59). In contrast, the segregate (also a place-defined cortical column) is composed of neurons with highly diverse RFs. In what respect then is the segregate an entity? The answer is provided by 3 experimental observations made both in the present study as well as in our previous study of the monkey's area 1 (Favorov and Whitsel, '88a). First, no systematic differences exist in the position of the maxRFs of neurons located in different sectors of a given segregate. Second, it is only at the point of the boundary separating 2 segregates that an en masse shift of maxRFs occurs; in other words, on the opposite sides of the boundary the maxRFs group about 2 displaced, nonoverlapping and noncontiguous skin loci. And third, the difference in the positions of the 2 groups of maxRFs mapped on opposite sides of a segregate boundary is large enough so that the segregate RF center of one segregate is included in only 53% of the maxRFs mapped within the other segregate. These 3 observations suggest that the segregate is an entity in a statistical sense: i.e., the different sectors of the same segregate have the same *distribution,* or assortment, of single neuron RFs. According to this view, the reason why adjacent segregates can be distinguished is because their RF distributions occupy different, and only partially overlapping skin territories.

The view of segregate organization proposed above assigns a particular meaning to the minRF. That is, in terms of the proposed framework the minRF method identifies one particular parameter of the distribution of maxRFs of the recorded neuronal population; i.e., the central tendency of the distribution. Thus the experimental finding that the same minRF is mapped at different cortical loci within the same segregate can be interpreted as indicating, in agreement with the above interpretation of the maxRF data, that maxRF distributions that obtain at different cortical loci within the same segregate exhibit the same central tendency. Furthermore, the experimental finding that minRF shifts abruptly at the boundary separating 2 segregates can be interpreted as indicating that segregate boundary separates 2 populations of neurons whose RF distributions exhibit different central tendencies.

Shape and size of segregates. The data indicate that sharp boundaries delineate each segregate. The 6 segregates mapped at high resolution in this study were each observed to be surrounded by 6 other segregates. Their cross-sectional shape was clearly not striplike, but rather that of an oval or a convex, only slightly elongated polygon. The size of a segregate apparently varies systematically with the position of its segregate RF center on the forelimb (i.e., segregates with RF centers located more distally on the forelimb are consistently larger than those with more proximally located RF centers). The size varied between 300 and 400 μm among segregates mapped with near-radial penetrations of the crown of the postsigmoid gyrus. However, segregates mapped with tangential penetrations of the medial bank of the coronal sulcus appeared to be significantly larger, close to 550 μm (Fig. 6). More significant than the width of a segregate is the number of neurons it contains, and in this regard it is unclear if the segregates in the sulcus were larger (i.e., contained more neurons) that segregates in the crown of the gyrus, since the thickness of the gray matter and the spacing of radial cords of cells can differ extensively between the gyrus crown and the sulcus wall.

Subdivisions within segregates. Pairwise analysis of maxRFs mapped within the same segregate reproduced an observation made previously in the monkey area 1 (Favorov and Whitsel, '88a): i.e., closely located neurons tended to have more similar maxRFs than did pairs separated by distances greater than 50 μm in the tangential cortical plane. As described in Results (see also Favorov and Whitsel, '88a,b), this outcome is consistent with the presence of subunits within a segregate—subunits consisting of vertically oriented groups of cells with heightened maxRF similarity. In other words, the maxRFs are more similar among neurons comprising a single vertical subunit than they are among neurons belonging to different subunits. In all likelihood the suggested subunits correspond to the radial cords of cells clearly seen in Nissl-stained sections of SI, and to "minicolumns," the basic modular units of the neocortex proposed by Mountcastle ('78).

How many minicolumns are in a segregate? The average cross-sectional area of a minicolumn is 1,750 μm^2 (this estimate is based on the assumption that a minicolumn has a shape of a 45 μm wide regular hexagon). Among the 6 segregates mapped at high resolution, the smallest one (shown in Fig. 4; its segregate RF center was on the proximal forearm) had an area of 0.072 mm^2. The largest mapped segregate (shown in Fig. 5; its segregate RF center was on digit 5) had an area of 0.14 mm^2. Based on these areal measurements, we suggest that segregates with RF centers on the forelimb contain between 40 and 80 minicolumns, depending on the proximo-distal position of the segregate RF center.

Generality of segregate organization. The picture of cat and monkey segregates developed above invites comparison with the barrel-based columns representing mystacial vibrissae in the SI of rats and some other rodent species. For example, both the vibrissae representation in the SI of those rodents and the forelimb representation in the cat SI are organized as mosaics of discrete topographic units, each unit receiving its strongest input from a single peripheral site (Woolsey and Van der Loos, '70; Welker, '71). The shape and size of segregates are similar to those of

barrels. In the absence of general anesthesia, neurons in both barrel-based columns and in segregates have a variety of RF sizes and configurations (Simons, '78; Simons and Woolsey, '79). Moreover, just as each barrel is associated with a principal whisker, which is included in the RFs of all its neurons, each segregate is associated with a single skin locus that is included in the RFs of all its neurons. The similarity of barrels and segregates of the cat and monkey SI, in 3 orders as phylogenetically distant from one another as are rodents, carnivores, and primates, suggests that segregation of the cortical representation of the body surface into discrete column-shaped units may be a general principle of mammalian cortical organization.

Segregates and mode-defined columns. In addition to segregates, discrete cortical columns have been identified in area 3b of the cat (Dykes and Gabor, '81; Sretavan and Dykes, '83) and monkey (Sur et al., '84) on the basis of the rate of adaptation of neural response to a maintained punctate stimulus. These slowly and rapidly adapting columns share the same cortical territory with segregates, raising the question of their positional relationships. In contrast to the honeycomb-like mosaic of segregates, submodality columns are arranged in a form of interdigitating, wavy bands; their width, however, is very similar to the width of segregates. Although neither group of investigators detected segregates, Dykes and Gabor ('81) observed that crossing the boundary separating slowly and rapidly adapting bands was sometimes accompanied by a jump of the RFs to a new body site. This report raises a provocative idea that (1) each segregate receives its input from mechanoreceptors of only one submodality, and (2) submodality bands in area 3b are composed of strings of segregates.

Mechanism of formation of segregates. There is a growing body of evidence that the body representation in SI of adult animals is maintained dynamically and reflects the nature and extent of environmental stimulation (for concise review, see Wall, '88). Can a rather uncomplicated epigenetic mechanism be responsible for the formation and maintenance of segregates? More specifically, could segregate organization result from a self-organizing process that begins at a very early stage of somatosensory cortical development within an initially homogeneously organized cortex? If such a process were operative, then segregates would not have to be genetically programmed but could be the natural outcome of the spatial patterns of synaptic weight modifications set up by early environmental stimulation.

The feasibility of such an epigenetic mechanism has been demonstrated by Edelman and colleagues (Pearson et al., '87). Using computer simulations of the SI cortical network, they showed that repeated sensory stimulation can profoundly reorganize a network that originally (at "birth") received somatotopically organized afferent input and possessed homogeneously organized intrinsic connections. For such a reorganization to take place, the afferent connections and the excitatory intrinsic connections had to be plastic, i.e., it was essential that the weights of the synaptic connections depend on the extent to which the pre- and postsynaptic activities were correlated (such a synaptic modification mechanism commonly has come to be referred to as *Hebbian*). As a result of repeated sensory stimulation, such an initially uniform, continuously connected 2-dimensional network came to be subdivided into a mosaic of small discrete regions having the following features: (1) the connections among neurons within each such region were strengthened, whereas connections among different regions were profoundly weakened, (2) the neurons within each region acquired identical or very similar focal RFs, and (3) the neurons in adjacent regions came to possess different, nonoverlapping RFs. In addition, the transition from one such region to its neighbor was marked by an abrupt shift of RFs to a new location. Edelman and colleagues identified these discrete regions as "neuronal groups" (Pearson et al., '87). Although in many respects these neuronal groups bear a striking resemblance to segregates, there are 2 critical differences. First, a neuronal group is predicted to occupy, in the tangential cortical plane, a territory 50 to 100 μm in diameter (Edelman and Finkel, '84)—an area much smaller than that occupied by a segregate. Even more importantly, neurons comprising a neuronal group are predicted to have very similar RFs (Edelman and Finkel, '84; Pearson et al., '87), an outcome due to the strong excitatory interconnections within a group, a defining feature of neuronal groups (Edelman, '78). In contrast, the neurons comprising a segregate have highly varied RFs.

Although neuronal groups differ substantially from the topographic units identified in the present study, the possibility remains that the parcelling mechanism described by Edelman and colleagues (Pearson et al., '87) can be adapted to provide a possible explanation of how the minicolumns of a homogeneously organized cortex (one at an early stage of development) might group together to form segregates, and how segregates might acquire their RF centers. This possibility is currently under examination in our laboratory.

ACKNOWLEDGMENTS

We thank Drs. Barry Whitsel and Irving Diamond for valuable discussions and comments on the manuscript, and Calvin Wong for expert technical assistance. The work was sponsored by NIH Grant DE07509. M.E.D. was supported by an NSF predoctoral fellowship.

LITERATURE CITED

Bennett, R.E., D.G. Ferrington, and M. Rowe (1980) Tactile neuron classes within second somatosensory area (SII) of cat cerebral cortex. J. Neurophysiol. *43*:292–309.

Chapin, J.K., and C.S. Lin (1984) Mapping the body representation in the SI cortex of anesthetized and awake rats. J. Comp. Neurol. *229*:199–213.

Duncan, G.H., D.A. Dreyer, T.M. McKenna, and B.L. Whitsel (1982) Dose- and time-dependent effects of ketamine on SI neurons with cutaneous receptive fields. J. Neurophysiol. *47*:677–699.

Dykes, R.W., and A. Gabor (1981) Magnification functions and receptive field sequences for submodality-specific bands in SI cortex of cats. J. Comp. Neurol. *202*:597–620.

Dykes, R.W., and A. Ruest (1981) What makes a map in somatosensory cortex? In E.G. Jones and A. Peters (eds): Cerebral Cortex, vol. 5. New York: Plenum Press, pp. 1–29.

Dykes, R.W., D.D. Rasmusson, and P.B. Hoeltzell (1980) Organization of primary somatosensory cortex in the cat. J. Neurophysiol. *43*:1527–1546.

Edelman, G.M. (1978) Group selection and phasic reentrant signalling: A theory of higher brain function. In G.M. Edelman and V.B. Mountcastle (eds): The Mindful Brain. Cambridge: MIT Press, pp. 51–100.

Edelman, G.M., and L.H. Finkel (1984) Neuronal group selection in the cerebral cortex. In G.M. Edelman, W.E. Gall, and W.M. Cowan (eds): Dynamic Aspects of Neocortical Function. New York: John Wiley & Sons, pp. 653–695.

Favorov, O., and B.L. Whitsel (1988a) Spatial organization of the peripheral input to area 1 cell columns: I. The detection of "segregates." Brain Res. Rev. *13*:25–42.

Favorov, O., and B.L. Whitsel (1988b) Spatial organization of the peripheral input to area 1 cell columns: II. The forelimb representation achieved by a mosaic of segregates. Brain Res. Rev. *13:*43–56.

Favorov, O.V., M.E. Diamond, and B.L. Whitsel (1987) Evidence for a mosaic representation of the body surface in area 3b of the somatic cortex of cat. Proc. Natl. Acad. Sci. USA *84:*6606–6610.

Felleman, D.J., J.T. Wall, C.G. Cusick, and J.H. Kass (1983) The representation of the body surface in S-I of cats. J. Neurosci. *3:*1648–1669.

Iwamura, Y., M. Tanaka, M. Sakamoto, and O. Hikosaka (1985) Diversity in receptive field properties of vertical neuronal arrays in the crown of the postcentral gyrus of the conscious monkey. Exp. Brain Res. *58:*400–411.

Jones, E.G. (1975) Varieties and distribution of non-pyramidal cells in the somatic sensory cortex of the squirrel monkey. J. Comp. Neurol. *160:*205–267.

Jones, E.G. (1981) Anatomy of cerebral cortex: Columnar input-output organization. In F.O. Schmitt, F.G. Worden, G. Edelman, and S.G. Dennis (eds): The Organization of the Cerebral Cortex. Cambridge: MIT Press, pp. 199–235.

Kaas, J.H., M. Sur, R.J. Nelson, and M.M. Merzenich (1981) The postcentral somatosensory cortex: Multiple representations of the body in primates. In C.N. Woolsey (ed): Cortical Sensory Organization, vol. 1. Clifton, NJ: Humana Press, pp. 29–45.

McKenna, T.M., B.L. Whitsel, and D.A. Dreyer (1981) Organization of cat anterior parietal cortex: Relations among cytoarchitecture, single neuron functional properties and interhemispheric connectivity. J. Neurophysiol. *45:*667–697.

McKenna, T.M., B.L. Whitsel, and D.A. Dreyer (1982) Anterior parietal cortical topographic organization in macaque monkey: A re-evaluation. J. Neurophysiol. *48:*289–317.

Marshall, W.H., C.N. Woolsey, and P. Bard (1937) Cortical representation of tactile sensibility as indicated by cortical potentials. Science *85:*388–390.

Merzenich, M.M., J.H. Kaas, M. Sur, and C.S. Lin (1978) Double representation of the body surface within cytoarchitectonic areas 3b and 1 in S-I in the owl monkey (*Aotus trivirgatus*). J. Comp. Neurol. *181:*41–74.

Merzenich, M.M., M. Sur, R.J. Nelson, and J.H. Kaas (1981) Organization of the SI cortex: Multiple cutaneous representations in areas 3b and 1 of the owl monkey. In C.N. Woolsey (ed): Cortical Sensory Organization, vol. 1. Clifton, NJ: Humana Press, pp. 47–66.

Mountcastle, V.B. (1957) Modality and topographic properties of single neurons of cat's somatic sensory cortex. J. Neurophysiol. *20:*374–434.

Mountcastle, V.B. (1978) An organizing principle for cerebral function: The unit module and the distributed system. In G.M. Edelman and V.B. Mountcastle (eds): The Mindful Brain. Cambridge: MIT Press, pp. 7–50.

Nelson, R.J., M. Sur, D.J. Felleman, and J.H. Kaas (1980) Representations of the body surface in postcentral parietal cortex of *Macaca fascicularis*. J. Comp. Neurol. *192:*611–643.

Pearson, J.C., L.H. Finkel, and G.M. Edelman (1987) Plasticity in the organization of adult cerebral cortical maps: A computer simulation based on neuronal group selection. J. Neurosci. *7:*4209–4223.

Powell, T.P.S., and V.B. Mountcastle (1959) Some aspects of the functional organization of the cortex of the postcentral gyrus of the monkey: A correlation of findings obtained in a single unit analysis with cytoarchitecture. Bull. Johns Hopkins Hosp. *105:*133–162.

Simons, D.J. (1978) Response properties of vibrissa units in rat SI somatosensory neocortex. J. Neurophysiol. *41:*798–820.

Simons, D.J., and T.A. Woolsey (1979) Functional organization in mouse barrel cortex. Brain Res. *165:*327–332.

Sretavan, D., and R.W. Dykes (1983) The organization of two cutaneous submodalities in the forelimb region of area 3b of cat somatosensory cortex. J. Comp. Neurol. *213:*381–398.

Sur, M., J.T. Wall, and J.H. Kaas (1984) Modular distribution of neurons with slowly adapting and rapidly adapting responses in area 3b of somatosensory cortex in monkeys. J. Neurophysiol. *51:*724–744.

Wall, J.T. (1988) Variable organization in cortical maps of the skin as an indication of the lifelong adaptive capacities of circuits in the mammalian brain. TIN *11:*549–557.

Weinberger, N.M., W. Hopkins, and D.M. Diamond (1984) Physiological plasticity of single neurons in auditory cortex of the cat during acquisition of the pupillary conditioned response: I. Primary field (AI). Behav. Neurosci. *98:*171–188.

Welker, C. (1971) Microelectrode delineation of fine grain somatotopic organization of SmI cerebral neocortex in albino rat. Brain Res. *26:*259–275.

Whitsel, B.L., J.R. Roppolo, and G. Werner (1972) Cortical information processing of stimulus motion on primate skin. J. Neurophysiol. *35:*691–717.

Woolsey, T.A., and H. Van der Loos (1970) The structural organization of layer IV in the somatosensory region (SI) of mouse cerebral cortex. Brain Res. *17:*205–242.